

ESR study in lightly doped $\text{La}_{1-x}\text{Sr}_x\text{MnO}_3$

V. A. Ivanshin ^a, J. Deisenhofer ^a, H.-A. Krug von Nidda ^a, A. Loidl ^a, A. A. Mukhin ^b, A.

M. Balbashov ^c, and M. V. Eremin ^d

^a *Experimentalphysik V, EKM, Universität Augsburg, 86135*

Augsburg, Germany

^b *Institute of General Physics, Russian Academy of Sciences, 117942*

Moscow, Russia

^c *Moscow Power Engineering Institute, 105835 Moscow, Russia*

^d *Kazan State University, 420008 Kazan, Russia*

(January 5, 2018)

Abstract

We present a systematic electron-spin-resonance (ESR) study in single crystals of $\text{La}_{1-x}\text{Sr}_x\text{MnO}_3$ ($0 \leq x \leq 0.2$). The temperature dependence of the ESR linewidth marks all significant transitions between both orthorhombic (O, O) and the rhombohedral (R) structural phases of the $T - x$ phase diagram. All significant peculiarities of the ESR spectra for low x values ($x \leq 0.125$) can be attributed to the cooperative Jahn-Teller effect on the Mn^{3+} e_g states and to the influence of the Dzyaloshinsky-Moriya exchange interaction. Possible relaxation mechanisms at higher doping levels are discussed.

PACS: 76.30.-v, 71.38.+i, 72.80.Ga, 75.70.Pa

I. INTRODUCTION

Due to the interplay of spin, charge, orbital, and lattice degrees of freedom the doped perovskite manganites ($\text{La}_{1-x}\text{Me}_x^{2+}\text{Mn}_{1-x}^{3+}\text{Mn}_x^{4+}\text{O}_3$; Me = Ca, Sr, Pb, and Ba [1]) reveal a variety of interesting phenomena, among which colossal magnetoresistance (CMR) [2,3], which also can be induced by an electric field [4], magnetic-field induced structural phase transitions [5] and photo-induced metal to insulator transitions [6] can be found. This variety of very unusual phenomena corresponds to a complex (x, B, T)-phase diagram exhibiting magnetic order, which strongly depends on the hole concentration [7,8], orbital order [8,9], charge order [10] and different structural phases, which depend on the tolerance factor and on long-range Jahn-Teller distortions [11]. The ground-state properties of the manganites arise from the orbital degeneracy with a strong Hund's coupling and are derived from a strong competence of super-exchange [8] and double-exchange [12] interactions and by the concomitant appearance of charge order and long-range Jahn-Teller distortions.

A phase diagram for $\text{La}_{1-x}\text{Sr}_x\text{MnO}_3$ for strontium-doping concentrations $x \leq 0.2$ has been published recently by Paraskevopoulos et al. [13]. In accordance to an early investigation [11] the sequence rhombohedral R to orthorhombic O (at a transition temperature of 1020 K) and then to another orthorhombic O' structure (at 760 K) was observed in pure LaMnO_3 , which is electrically insulating and displays antiferromagnetic ordering of the Mn^{3+} ions at the Neel temperature $T_N = 140$ K. The three octahedral Mn-O lengths are strongly anisotropic in the O' phase, due to a long-range Jahn-Teller distortion, and become almost equal in the O phase. With increasing doping concentration x the conductivity of the manganites increases. This can be attributed to the growing amount of holes in the lattice on Mn^{4+} sites. Owing to the strong Hund's coupling, the hopping of an e_g electron between Mn^{3+} and Mn^{4+} sites is the dominating mechanism for the conductivity of manganites in the paramagnetic regime [15]. Driven by an increasing concentration of mobile holes, at low temperatures the insulating and antiferromagnetic (AFM) structure passes to a purely metallic and ferromagnetic state for $x > 0.17$. Close to $x = 1/8$ the ground state is a fer-

romagnetic (FM) insulator. The Jahn-Teller distortions of the O' phase become suppressed for $x > 0.15$, where the undistorted O phase extends to the lowest temperatures. The competition between ferromagnetism and antiferromagnetism causes a complicated ground state. At the moment, the coexistence of antiferromagnetic spin correlations along with the conventional ferromagnetic spin correlations is explained either within the framework of a canted antiferromagnetic (CA) state or with a mixed two-phase state. The existence of a phase separation was reported in the lightly doped $\text{La}_{1-x}\text{Sr}_x\text{MnO}_3$ samples from a computational analysis in the framework of the two-orbital Kondo model with Jahn-Teller polarons [16]. A phase separation was found to occur between (i) hole-undoped antiferromagnetic and hole-rich paramagnetic regions and (ii) antiferromagnetic and ferromagnetic phase with low, respectively high, hole concentration. Recent neutron scattering [10], optical [17], and NMR [18] measurements on manganites can be interpreted in the framework of this theoretical model.

The perovskite manganites show intense electron-spin-resonance (ESR) signals with a large variation of the ESR-line parameters as a function of the temperature [14]. Several controversial approaches have been made to explain the ESR data in manganites. In the paramagnetic state the ESR spectrum consists of a single resonance line with a g value near 2.0. The broad ESR line in pure LaMnO_3 (ESR linewidth $\Delta H \sim 2.5$ kOe at room temperature) was ascribed to Mn^{3+} [19]. The linear temperature dependence of the linewidth in $\text{La}_{0.67}\text{Sr}_{0.33}\text{MnO}_3$ and $\text{La}_{0.62}\text{Bi}_{0.05}\text{Ca}_{0.33}\text{MnO}_3$ was related to contributions from spin-phonon relaxation [20]. The characteristic differences observed in ESR intensity and linewidth in $\text{La}_{1-x}\text{Ca}_x\text{MnO}_3$ ($x=0.1; 0.2$) ceramic samples were attributed to a model, in which a bottlenecked spin relaxation takes place from Mn^{4+} ions via Mn^{3+} Jahn-Teller ions to the lattice [21]. The authors argue that the ESR signal is due to Mn^{4+} only, but renormalized by the exchange coupling to Mn^{3+} . In ref. [22] it was found that all Mn spins contribute to the ESR signal in $\text{La}_{1-x}\text{Sr}_x\text{MnO}_3$ ($x = 0.1; 0.2; 0.3$) single crystals. The authors suggest that the linewidth increases linearly as a result of spin-lattice relaxation involving a single phonon. Finally, Causa et al. [14] showed that all Mn spins contribute to the resonance in perovskite

compounds $A_{0.67}Me_{0.33}MnO_3$ ($A = La, Pr$; $Me = Ca, Sr$) due to spin-spin interactions, and not only the Mn^{4+} or some spin clusters, with no evidence of a spin-phonon contribution to the experimental linewidth. Therefore, it is very important to perform ESR measurements on manganites in an extended concentration and temperature range in order to clarify the situation and to correlate the results with different theoretical models. There are extremely few publications devoted to the ESR studies on manganites in the low doped region with only several doping concentrations of $x \leq 0.2$ [21–24].

In the present paper we report on our systematic ESR study in $La_{1-x}Sr_xMnO_3$ ($x = 0; 0.05; 0.075; 0.1; 0.125; 0.15; 0.175; 0.2$) single crystals in the paramagnetic regime in attempt to compare the temperature dependence of the width and intensity of the ESR lines with a detailed and complete phase diagram (see Fig. 1), which was established recently in the same samples after electrical conductivity, magnetic susceptibility, submillimeter permittivity, and dynamic conductivity investigations [25,13]. Particular attention is devoted to the discussion of the linewidth in the Jahn-Teller distorted phase.

II. EXPERIMENTAL

Single crystals of $La_{1-x}Sr_xMnO_3$ were grown by the floating-zone method with radiation heating in air atmosphere, as described in ref. [25]. The purity of the chemicals used for sample preparation (La_2O_3 , $SrCO_3$ and Mn_3O_4) was not less than 99.99%. X-ray powder diffraction proved that the grown materials were of single phase. However, two dimensional X-ray TV topography of the crystals has revealed a twin structure.

ESR measurements were performed with a Bruker ELEXSYS E500 CW-spectrometer at X-band frequencies ($\nu \approx 9.2$ GHz) equipped with continuous gas-flow cryostats for He (Oxford Instruments) and N_2 (Bruker) in the temperature range between 4.2 K and 680 K. Small crystals of 0.6 - 3.7 mg were chosen for our ESR experiments to avoid the sample-size effects [14]. The samples were placed into quartz tubes and fixed with either paraffin (at low temperatures $4\text{ K} \leq T \leq 300\text{ K}$) or NaCl (at $300\text{ K} \leq T \leq 680\text{ K}$). We have restricted our

experiments to the paramagnetic regime ($T > T_N$) only, because within the magnetically ordered regime the ESR behavior is very sample dependent, which is attributed to magnetic inhomogeneity of the samples in the antiferromagnetic and ferromagnetic phases due to local variations of oxygen stoichiometry and chemical composition [14,22].

A. ESR spectra

Electron-spin resonance detects the power P absorbed by the sample from the transverse magnetic microwave field as a function of the static magnetic field H . The signal-to-noise ratio of the spectra is improved by recording the derivative dP/dH with lock-in technique. ESR spectra, which are characteristic for the three structural phases of the paramagnetic regime, are presented in Fig. 2, illustrating their evolution with Sr concentration x (left column) and temperature T (right column). Within the whole paramagnetic regime the spectrum consists of a broad, exchange narrowed resonance line, which is well fitted by a Dysonian line shape [26]. As the linewidth ΔH is of the same order of magnitude as the resonance field H_{res} in the present compounds, one has to take into account both circular components of the exciting linearly polarized microwave field. Therefore the resonance at the reversed magnetic field $-H_{res}$ has to be included into the fit formula for the ESR signal, given by

$$\frac{dP}{dH} \propto \frac{d}{dH} \left(\frac{\Delta H + \alpha(H - H_{res})}{(H - H_{res})^2 + \Delta H^2} + \frac{\Delta H + \alpha(H + H_{res})}{(H + H_{res})^2 + \Delta H^2} \right) \quad (1)$$

This is an asymmetric Lorentzian line, which includes both absorption and dispersion, where α denotes the dispersion-to-absorption ratio. Such asymmetric line shapes are usually observed in metals, where the skin effect drives electric and magnetic microwave components out of phase in the sample and therefore leads to an admixture of dispersion into the absorption spectra. For samples small compared to the skin depth one expects a symmetric absorption spectrum ($\alpha = 0$), whereas for samples large compared to the skin depth absorption and dispersion are of equal strength yielding an asymmetric resonance line ($\alpha = 1$).

At low Sr concentrations or at low temperatures the spectra are nearly symmetric with respect to the resonance field in accordance with pure absorption spectra with $\alpha=0$. With increasing x or T they become more and more asymmetric corresponding to an increasing parameter α . To check, whether the skin effect is the reason for the asymmetric line shape, we have to estimate the skin depth $\delta = (\rho/\mu_0\omega)^{0.5}$ from the electric resistance ρ and the microwave frequency $\omega = 2\pi \times 9$ GHz ($\mu_0 = 4\pi \times 10^{-7}$ Vs/Am). Using the resistance values determined by Mukhin [25] - for example $\rho = 0.2$ Ω cm for $x = 0.125$ at room temperature - we find a skin depth $\delta = 0.16$ mm. Within the whole paramagnetic regime, the resistance values decrease by at least two orders of magnitude with increasing temperature or increasing Sr concentration. Therefore the skin depth is larger than the sample dimensions at low T or x and becomes comparable to or even smaller than the thickness of the sample as these parameters increase in accordance with the increasing asymmetry of the ESR spectra.

The resonance field of all compounds under investigation yields a g value slightly below the free-electron value, which is usual for transition-metal ions with a less than half filled d shell [27]. This g value is found to be nearly isotropic $g \approx 1.98$ in both the orthorhombic O and the rhombohedral R phase, but it reveals a weak anisotropy $1.94 \leq g \leq 1.98$ within the Jahn-Teller distorted O' phase. Finally approaching the ordering temperature from above, the whole resonance becomes seriously distorted and is strongly shifted to lower or higher fields dependent on the orientation of the sample. This is caused by internal fields due to the onset of magnetic order. More detailed information on the different phases is obtained from the resonance linewidth and the ESR intensity, which are presented in the following subsection.

B. Temperature dependence of the ESR linewidth and intensity

In Fig. 3 the ESR linewidth ΔH is plotted versus temperature for all investigated samples. Here the orientation of the single crystals was adjusted to the most pronounced temperature dependence, which could be found within the Jahn-Teller distorted O' phase

and is described in more detail below. Only for the pure sample $x = 0$ it was impossible to find an unequivocal orientation as it is presumably a twinned crystal. On the other hand, the crystals with Sr concentrations $x \geq 0.15$ had not been oriented, because they never reach the Jahn-Teller distorted regime and their paramagnetic spectra are isotropic.

The magnitude of ΔH is approximately constant in the whole temperature range $150 \text{ K} < T < 650 \text{ K}$ in pure LaMnO_3 , because the structural transition into the O phase takes place close to 800 K [25]. However, in all doped samples the temperature dependence of ΔH exhibits a number of deviations from a monotonic behavior, which we identified with different magnetic and structural phase transitions. At lowest temperatures of observation ($150 \text{ K} < T < 200 \text{ K}$) ΔH passes a minimum, as the temperature approaches T_N from above, and then increases abruptly near T_N . This dependence indicates the transition from the paramagnetic regime into the magnetically ordered structure and is connected with the strong shift of the resonance field mentioned above. The typical features of the linewidth obtained within the different paramagnetic regimes can be summarized as follows:

(a) Orthorhombic strongly Jahn-Teller distorted O' phase: A strongly anisotropic linewidth was observed in the lightly doped samples with $x \leq 0.125$. Fig. 4 depicts the temperature dependence of the linewidth for the three main orientations of the external magnetic field H in $\text{La}_{0.95}\text{Sr}_{0.05}\text{MnO}_3$. If the magnetic field is found within the a-b plane, the linewidth passes a maximum with increasing temperature, whereas the linewidth remains nearly constant, if the field is parallel to the c axis. At $T = 600 \text{ K}$, where the structural transition to the O phase takes place, the values of ΔH coincide for all directions. The angular dependence of the linewidth, which is shown in Fig. 5, can be commonly described by $A + B \sin^2 \vartheta$. At the temperature of maximal anisotropy ($T = 400 \text{ K}$) we found the ratio $B/A = 0.56$.

(b) Orthorhombic O phase: The upper temperature limit of the anisotropy in the linewidth is changing in the Sr doped samples from 600 K ($x = 0.05$) to 260 K ($x = 0.125$). This coincides quite well with the $O' \rightarrow O$ transition from the strongly Jahn-Teller distorted orthorhombic structure to the weakly distorted orthorhombic pseudocubic one. In

this phase, the linewidth ΔH exhibits a linear temperature dependence with a typical slope of about 2 Oe/K.

(c) Rhombohedral R phase: Again, a linear temperature dependence of the linewidth is observed for all samples investigated in this phase ($0.075 \leq x \leq 0.2$) up to 600 K. Its slope is comparable to the O phase. For $x < 1.5$ there is a slight kink at the $O \rightarrow R$ transition. Finally, the data points at the highest temperatures of this investigation ($600\text{K} < T < 680\text{K}$) indicate a tendency to saturation of ΔH .

The integrated intensity $I(T)$ of the resonance line measures the spin susceptibility χ_{ESR} of the ESR probe. For ferromagnetically coupled ions its temperature dependence usually follows a $(T - \Theta_{cw})^{-1}$ Curie-Weiss law, where Θ_{CW} is the Curie-Weiss temperature. If all spins take part in producing the ESR signal, it is reasonable to plot $1/I$ versus T and to expect a linear behavior all over the paramagnetic regime. However, as one can obtain from Fig. 6, this procedure does not yield a unique linear temperature dependence at all. Only LaMnO_3 behaves linearly with a Curie-Weiss temperature $\Theta_{CW}(x = 0) \approx 87$ K in the complete temperature range under consideration. For Sr concentrations $0.05 \leq x \leq 0.125$ we observe a distinct kink near the structural phase transition $\mathcal{O} \rightarrow O$, just at the temperature where the anisotropy of the linewidth starts to decrease with increasing temperature. Below this kink, the inverse intensity shows a linear temperature dependence with a similar slope as in LaMnO_3 . The respective Curie-Weiss temperatures increase with increasing Sr concentration up to $\Theta_{CW}(x = 0.125) \approx 208$ K. To analyze the origin of the ESR signal, we compared its intensity at temperatures below the kink to the ESR intensity of the so called green phase $\text{Gd}_2\text{BaCuO}_5$, which exhibits an ESR signal with a similar linewidth. The respective compound, in which all Gd^{3+} spins contribute to the ESR signal, shows a Curie-Weiss susceptibility with $\Theta_{CW} = -23$ K [28]. Starting with pure LaMnO_3 , we found that all Mn^{3+} ions contribute to the ESR signal with their full magnetic moment in the \mathcal{O} phase. With increasing Sr concentration x the averaged magnetic moment of both Mn^{3+} and Mn^{4+} ions even increases slightly by nearly 10 percent up to $x = 0.125$ within this phase, although Mn^{4+} ions (spin $S = 3/2$) exhibit a smaller magnetic moment than Mn^{3+}

ions (spin $S = 2$). Above the kink the inverse intensity again reaches a linear temperature dependence with a remarkably higher slope than below the kink (about 13 and 8 times the low-temperature slope for $x = 0.05$ and 0.1 respectively). As the inverse slope measures the total number of spins, which generate the ESR signal, about 90 percent of the spins seem to become invisible at the transition to the O phase, suggesting that the contribution of all Mn^{3+} ions disappears. However, we have to take the skin effect into account once more. Comparing the temperature of the kink in the intensity with the resistance data [25], we realize that it approximately coincides with the temperature, where the specific resistance drops below $1 \Omega \text{ cm}$ with increasing temperature. This corresponds to a skin depth of about 0.4 mm , which is of the order of the sample size. Therefore, the part of the crystal, which is accessible for the microwave field and contributes to the ESR signal, is more and more reduced with increasing temperature. To check the importance of the skin effect in our experiments, we investigated a powder sample with a Sr concentration $x = 0.1$. Its inverse ESR intensity still showed a discontinuity at the phase transition $O' \rightarrow O$ but at higher temperatures it attained nearly the same slope as at low temperatures, indicating that all Mn spins contribute to the ESR signal in the O phase, as well.

III. DISCUSSION

A. Intensity of ESR

Before we analyze the linewidth data in detail, we first focus on the ESR intensity in order to show that its temperature dependence is in accordance with the behavior expected for Mn^{3+} within an intermediate octahedral ligand field under the influence of distortion [27]: The octahedral field splits the five d orbitals into a lower triplet t_{2g} and an upper doublet e_g with an energy splitting of about 10^4 K . In the case of intermediate ligand fields the dominating Hund's coupling causes a parallel spin alignment of the four d electrons, where three of them occupy the triplet t_{2g} and the fourth is found in the doublet e_g (so called

high-spin state $S=2$). Therefore the ground state is an orbital doublet Γ_3 . Including the spin, the Γ_3 state is tenfold degenerated. This degeneration is lifted by second order spin-orbit couplings into a manifold of singlet, doublet, and triplet states with an overall splitting of about 20 K [27]. For this case the Zeeman effect is very complicated and the observation of an ESR signal is rather unlikely. The situation changes drastically for a tetragonal Jahn-Teller distortion, which splits the orbital doublet Γ_3 into two singlets with a typical energy gap of the order 10^3 K. Then the ground state is a spin quintuplet with usual Zeeman effect. Taking the spin-orbit coupling into account, the ESR signal is expected at about $g_z \approx 1.95$ and $g_x = g_y \approx 1.99$ [27], which agrees very well with our experimental data. In the case of Mn^{4+} in an octahedral field, the three d electrons occupy the triplet t_{2g} with parallel spin alignment $S = 3/2$. The ground state is an orbital singlet Γ_2 with a spin quadruplet. This yields an ESR signal with an isotropic g value at about $g \approx 1.99$.

Therefore the ESR signal is due to all Mn^{3+} and Mn^{4+} spins within the Jahn-Teller distorted \mathcal{O} phase. The increase of the averaged moment with the Sr concentration x , which is found in contrast to the expected linear superposition of Mn^{3+} and Mn^{4+} spins, agrees with susceptibility measurements [13] and may be ascribed to ferromagnetic polarization around the Mn^{4+} spins. With suppression of the Jahn-Teller distortion at the transition $\mathcal{O} \rightarrow O$ the contribution of the Mn^{3+} ions should vanish, if their surrounding is ideally octahedral. Obviously the weak orthorhombic distortion of the O phase is still strong enough to retain the ESR signal of Mn^{3+} .

B. Linewidth

The result that the Jahn-Teller Mn^{3+} ions dominate the ESR signal within the \mathcal{O} phase is essential for the following discussion of the linewidth within this regime: All significant peculiarities of the ESR spectra in the respective phase, i. e. the magnitude of the ESR linewidth, its anisotropy, and the anisotropy of the resonance field, are very similar to those observed by Tanaka et al. [29] in the quasi-one dimensional compound CsCuCl_3 . That system

exhibits a cooperative Jahn-Teller effect in the temperature range between 120 K and 560 K. The authors explain their ESR results due to Dzyaloshinsky-Moriya (DM) antisymmetric interaction [30] between Jahn-Teller Cu^{2+} ions i and j , given by

$$\mathcal{H}_{ij} = \mathbf{D}_{ij} \cdot [\mathbf{S}_i \times \mathbf{S}_j]. \quad (2)$$

ESR investigations in KCuF_3 [31] and CuGeO_3 [32], which are quasi-one dimensional systems as well, have been treated in a similar way. In those publications it was shown that the usual dipolar or anisotropic exchange interactions cannot produce the observed linewidth of the order of 10^3 Oe, because the strong exchange interaction between the Cu^{2+} ions leads to a considerable narrowing of the ESR line. The present compound $\text{La}_{1-x}\text{Sr}_x\text{MnO}_3$ exhibits comparable exchange interactions between Mn^{3+} ions (for $x = 0$) with spin $S = 2$ and between Mn^{3+} and Mn^{4+} ions with $S = 3/2$ (for $x > 0$). Therefore, we suggest that the broad ESR line in the strongly Jahn-Teller distorted O' phase of LaMnO_3 can be interpreted in terms of the DM antisymmetric interaction [30] between Mn^{3+} ions, which are strongly super-exchange coupled via oxygen ions. The dominance of the antisymmetric interactions in the Jahn-Teller distorted phase is also confirmed by the fact that non-Jahn-Teller Mn^{4+} ions suppress the line-broadening for $x > 0.125$. This finding supports the suggestion of Millis [33] that strong coupling between charges and lattice is observed in the Sr doped manganites due to the cooperative Jahn-Teller effect for Sr concentrations less than $x \approx 0.15$.

Looking at the magnetic structure [34] of the antiferromagnetic phase (see Fig. 7), one recognizes that each Mn^{3+} ion is coupled ferromagnetically to its four next Mn^{3+} neighbors within the a-b plane and antiferromagnetically to the other two in direction of the c axis. Therefore the compound is quasi-one dimensional along the antiferromagnetically coupled Mn^{3+} chains in c direction, and the analysis can be performed similar to the compounds cited above. Following Yamada [31], for temperatures $k_B T$ large compared to the exchange interaction J between the Mn ions, the linewidth contribution ΔH_{DM} of the DM interaction is approximated by

$$\Delta H_{DM} = \frac{\mathbf{D}_{ij}^2 S(S+1)}{6g\mu_B J} f(\vartheta), \quad (3)$$

where $f(\vartheta) = (1 + \cos^2 \vartheta)/4$ for \mathbf{D}_{ij} parallel or $f(\vartheta) = (2 + \sin^2 \vartheta)/8$ for \mathbf{D}_{ij} perpendicular to the quasi-one dimensional chain direction. Furthermore the g-shift $\Delta g = g - 2$ is given by

$$\Delta g = \frac{D}{2J} g, \quad (4)$$

where D and g denote the absolute value of \mathbf{D}_{ij} and the mean value of the anisotropic g tensor, respectively.

From Fig. 4 and Fig. 5 we obtain that for high temperatures $T > 300$ K the linewidth changes only slightly within the a-b plane but is strongly anisotropic with respect to the c axis following a $\sin^2 \vartheta$ law. As it is shown in the insert of Fig. 4, the anisotropy reaches a maximum value of $\Delta H_a/\Delta H_c = 1.56$. This agrees quite well with the expected value of 1.5 for $f(\vartheta) = (2 + \sin^2 \vartheta)/8$. So the vector \mathbf{D}_{ij} is pointing perpendicular to the quasi-one dimensional chain direction. To identify the origin of the DM interaction in the present system and to estimate its magnitude, we have to take into account the distortions of the crystal structure (see Fig. 7). Indeed, according to microscopic theory [35,36], one obtains

$$\mathbf{D}_{ij} = \mathbf{D}_O \cdot [\mathbf{n}_{iO} \times \mathbf{n}_{Oj}], \quad (5)$$

where \mathbf{n} are unit vectors along $\text{Mn}^{3+}\text{-O}^{2-}$ bonds. In LaMnO_3 these bonds are found along the chain direction [34], as indicated in Fig. 7, and the bridge angle ϕ is about 155° . Therefore the vector product $[\mathbf{n}_{iO} \times \mathbf{n}_{Oj}]$ does not vanish and \mathbf{D}_{ij} is perpendicular to the $\text{Mn}^{3+}\text{-O}^{2-}\text{-Mn}^{3+}$ triangle plane and to the chain axis. Taking into account the Jahn-Teller effect at the Mn^{3+} site, we conclude that the super-exchange coupling is mainly realized via $3z^2 - r^2$ orbitals of the Mn^{3+} ions. The situation is very similar to that which occurs in RFeO_3 , where R denotes a rare-earth ion, because the orbitals $x^2 - y^2$ are not active in the super-exchange coupling of $\text{Fe}^{3+}\text{-O}^{2-}\text{-Fe}^{3+}$, too. Using the channel model [37], we get

$$J_{\text{Mn}^{3+}\text{-O}^{2-}\text{-Mn}^{3+}} = \frac{S_{\text{Fe}^{3+}}^2}{S_{\text{Mn}^{3+}}^2} J_{\text{Fe}^{3+}\text{-O}^{2-}\text{-Fe}^{3+}} \quad (6)$$

Furthermore we can estimate the parameter of the DM interaction in the same manner [38]

$$D_{Mn^{3+}-O^{2-}-Mn^{3+}} = \frac{S_{Fe^{3+}}^2}{S_{Mn^{3+}}^2} D_{Fe^{3+}-O^{2-}-Fe^{3+}} \quad (7)$$

Using the data for Fe^{3+} from ref. [36] and taking into account the dependencies of J and D on the bridge angle ϕ we finally get for Mn^{3+} $J = 67$ K and $D = 2.54$ K. With these values we estimate the expected g-shift $\Delta g = 0.04$ and linewidth $\Delta H = 2.15$ kOe, which agree quite well with the experimental results.

Finally we shortly comment on the temperature dependence of the linewidth in both O and R phases, which has been discussed controversially by several authors as mentioned in the introduction. For intermediate Sr concentrations $0.075 \leq x \leq 0.15$ the linear increase of the linewidth may be due to the spin-lattice relaxation, as it was suggested in ref. [22], because of the importance of electron-phonon interactions at this doping level [40]. Nevertheless, the quasi-linear behaviour of ΔH at $x > 0.15$ is also well described by a model on the basis of effective Heisenberg-like interactions for Mn^{3+} - Mn^{4+} spin pairs with no evidence of spin-phonon contribution to the experimental linewidth [14]. The infinite-temperature linewidth for different doped manganites with Me-concentration $x = 0.33$ observed in the latter study up to 1000 K was kept as adjustable parameter, which is related to spin-only interactions.

Very recent studies of Shengelaya et al. [41] notice the similarity between temperature dependence of ESR linewidth and conductivity in manganites, which is determined by the hopping motion of small polarons [15]. Quasioptical spectroscopy measurements on the same samples as in our studies reveal that hopping or tunneling between localized states dominates the conductivity for Sr concentrations $x \leq 0.15$ and temperatures $T < 300$ K [42]. Even for $La_{0.825}Sr_{0.175}MnO_3$ the localization effects are observed at least 10 K below the magnetic phase transition. Therefore, one can support that the hopping rate of e_g charge carriers defines a broadening dynamics of the ESR line.

IV. CONCLUSION

We performed systematic ESR investigations on $\text{La}_{1-x}\text{Sr}_x\text{MnO}_3$ single crystals for Sr concentrations ($0 \leq x \leq 0.2$) within the paramagnetic regime. The ESR properties of the strongly Jahn-Teller distorted O' phase have been investigated in detail for the first time. Comparing the ESR intensity with $\text{Gd}_2\text{BaCuO}_5$, we obtained that the strongly exchange narrowed paramagnetic resonance is due to both Mn^{3+} and Mn^{4+} ions within both the strongly Jahn-Teller distorted O' phase and the weakly distorted pseudocubic O phase. The temperature dependence of the ESR linewidth marks all significant transitions between the structural phases of the $T - x$ phase diagram. Within the Jahn-Teller distorted O' phase, its magnitude and anisotropy are well understood in terms of the exchange modulation of the Dzyaloshinsky-Moriya antisymmetric interaction. The linewidth directly probes the suppression of the Jahn-Teller distortion with increasing Sr concentration and increasing temperature. In principle it should be possible to obtain the distortion angle from these data. However, further theoretical effort is necessary to describe the detailed temperature and concentration dependence of the ESR parameters under Jahn-Teller distortion.

ACKNOWLEDGEMENTS

We thank B. Elschner, B. I. Kochelaev, V. K. Voronkova, A. E. Usachev, A. Shengelaya and K. Held for useful discussions. This work was supported by the Bundesministerium für Bildung und Forschung (BMBF) under Contract No. 13N6917/0. M. V. Eremin was supported in part by the Russian Foundation for Basic Research, Grant No. 97-02-18598.

REFERENCES

- [1] G. H. Jonker and J. H. van Santen, *Physica* **16**, 337 (1950).
- [2] R. M. Kusters, D. A. Singleton, R. Mcgreevy, and W. Hayes, *Physica* **B 155**, 362 (1989).
- [3] R. von Helmolt, J. Wecker, B. Holzapfel, L. Schultz, and K. Samwer, *Phys. Rev. Lett.* **71**, 2331 (1993); K. Chahara, T. Ohno, M. Kasai, and Y. Kozono, *Appl. Phys. Lett.* **63**, 1990 (1993); S. Jin, T. H. Tiefel, M. McCormack, R. A. Fastnacht, R. Ramesh, and L. H. Chen, *Science* **264**, 413 (1994).
- [4] A. Asamitsu, Y. Tomioka, H. Kuwahara, and Y. Tokura, *Nature (London)*, **388**, 50 (1997).
- [5] Y. Tomioka, A. Asamitsu, H. Kuwahara, Y. Morimoto, and Y. Tokura, *Phys. Rev.* **B 53**, R1689 (1996).
- [6] K. Miyano, T. Tanaka, Y. Tomioka, and Y. Tokura, *Phys. Rev. Lett.* **78**, 4257 (1997).
- [7] P. G. de Gennes, *Phys. Rev.* **118**, 141 (1960).
- [8] J. B. Goodenough, A. Wold, R. J. Arnott, and N. Menyuk, *Phys. Rev.* **124**, 373 (1961).
- [9] Y. Murakami, J. P. Hill, D. Gibbs, M. Blume, I. Koyama, M. Tanaka, H. Kawata, T. Arima, Y. Tokura, K. Hirota, and Y. Endoh, *Phys. Rev. Lett.* **81**, 582 (1998).
- [10] Y. Yamada, O. Nino, S. Nohdo, R. Kanao, T. Ihami, and S. Katano, *Phys. Rev. Lett.* **77**, 904 (1996).
- [11] A. K. Bogush, V. I. Pavlov, and L. V. Balyko, *Cryst. Res. Technol.* **18**, 589 (1983).
- [12] C. Zener, *Phys. Rev.* **82**, 403 (1951); P. W. Anderson and H. Hasegawa, *Phys. Rev.* **100**, 675 (1955).
- [13] M. Paraskevopoulos, J. Hemberger, A. Loidl, A. A. Mukhin, V. Yu. Ivanov, and A. M. Balbashov, to be published in *J. Mag. Mag. Mat.* (1999).

- [14] M. T. Causa, M. Tovar, A. Caneiro, F. Prado, G. Ibanez, C. A. Ramos, A. Butera, B. Alascio, X. Obradors, S. Pinol, F. Rivadulla, C. Vazquez-Vazquez, M. A. Lopez-Quintela, J. Rivas, Y. Tokura, and S. B. Oseroff, *Phys. Rev.* **B 58**, 3233 (1998).
- [15] M. Jaime, H. T. Hardner, M. B. Salamon, M. Rubinstein, P. Dorsey, and D. Emin, *Phys. Rev. Lett.* **78**, 951 (1997).
- [16] S. Yunoki, J. Hu, A. L. Malvezzi, A. Moreo, N. Furukawa, E. Dagotto, *Phys. Rev. Lett.* **80**, 845 (1998).
- [17] J. H. Jung, K. H. Kim, H. J. Lee, J. S. Ahn, N. J. Hur, T. W. Noh, M. S. Kim, J.-G. Park, *Phys. Rev.* **B 59**, 3793 (1999).
- [18] G. Papavassiliou, M. Fardis, M. Belesi, M. Pissas, I. Panagiotopoulos, G. Kallias, D. Niarchos, C. Dimitropoulos, J. Dolinsek, *Phys. Rev.* **B 59**, 6390 (1999).
- [19] E. Granado, N. O. Moreno, A. Garcia, J. A. Sanjurjo, C. Rettori, I. Torriani, S. B. Oseroff, J. J. Neumeier, K. J. McClellan, S.-W. Cheong, and Y. Tokura, *Phys. Rev.* **B 58**, 11435 (1998).
- [20] M. S. Seehra, M. Ibrahim, V. S. Babu, and G. Srinivasan, *J. Phys.: Condens. Matter* **8**, 11283 (1996).
- [21] A. Shengelaya, G. Zhao, H. Keller, and K. A. Müller, *Phys. Rev. Lett.* **77**, 5296 (1996).
- [22] S. E. Lofland, P. Kim, P. Dahiroc, S. M. Bhagat, S. D. Tyagi, S. G. Karabashev, D. A. Shulyatev, A. A. Arsenov, and Y. Mukovskii, *Physics Letters A* **233**, 476 (1997).
- [23] C. Rettori, D. Rao, J. Singley, D. Kidwell, S. B. Oseroff, M. T. Causa, J. J. Neumeier, K. J. McClellan, S.-W. Cheong, and S. Schultz, *Phys. Rev.* **B 55**, 3083 (1997).
- [24] K. V. Baginskiĭ, V. A. Aleshin, V. A. Tulin, A. A. Arsenov, D. A. Shulyatev, and Ya. M. Mukovskiĭ, *JETP Letters* **67**, 1059 (1998).
- [25] A. A. Mukhin, V. Yu. Ivanov, V. D. Travkin, S. P. Lebedev, A. Pimenov, A. Loidl, and

- A. M. Balbashov, JETP Letters, **68**, No.4, 356 (1998).
- [26] G. Feher and A. F. Kip, Phys. Rev. **98**, 337 (1955).
- [27] A. Abragham and B. Bleaney, EPR of Transition Ions, Clarendon Press, Oxford 1970.
- [28] G. F. Goya, R. C. Mercader, L. B. Steren, R. D. Sanchez, M. T. Causa, and M. Tovar, J. Phys.: Condens. Matter **8**, 4529 (1996).
- [29] H. Tanaka, K. Iio, and K. Nagata, J. Phys. Soc. Jpn., **54**, 4345 (1985).
- [30] T. Moriya, Phys. Rev. Lett. **4**, 228 (1960); Phys. Rev. **120**, 91 (1960).
- [31] I. Yamada, H. Fujii, and M. Hidaka, J. Phys.: Condens. Matter **1**, 3397 (1989).
- [32] I. Yamada, M. Nishi, and J. Akimitsu, J. Phys.: Condens. Matter **8**, 2625 (1996).
- [33] A. J. Millis, Phys.Rev. **B 53**, 8434 (1996).
- [34] Q. Huang, A. Santoro, J. W. Lynn, R. W. Erwin, J. A. Borchers, J. L. Peng, and R. L. Greene, Phys. Rev. **B 55**, 14987 (1997).
- [35] F. Keffer, Phys. Rev. **126**, 896 (1962).
- [36] A. S. Moskvin and I. G. Bostrem, Sov. Phys. Solid State **19**, 1532 (1977).
- [37] M. V. Eremin, Yu. V. Rakitin, phys. stat. sol. (b) **80**, 579 (1977); M. V. Eremin, Yu. V. Rakitin, phys. stat. sol. (b) **82**, 227 (1977); M. V. Eremin, Yu. V. Rakitin, phys. stat. sol. (b) **85**, 783 (1977).
- [38] M. V. Eremin in Spectroscopiya crystallov (in Russian), ed.by A. A. Kaplyanskii, Nauka, Leningrad (1980), pp. 150-170.
- [39] B. I. Kochelaev, L. Kan, B. Elschner, and S. Elschner, Phys. Rev. **B 49**, 13106 (1994)
- [40] S. Uhlenbruck, R. Teipen, R. Klingeler, B. Büchner, O. Friedt, M. Hücker, H. Kierspel, T. Niemöller, L.Pinsard, A. Revcolevschi, and R. Gross, Phys.Rev.Lett. **82**, 185 (1999).

- [41] A. Shengelaya, G. Zhao, H. Keller, K. A. Müller, and B. I. Kochelaev, submitted to Phys. Rev. B. (1999)
- [42] A. Pimenov, Ch. Hartinger, A. Loidl, A. A. Mukhin, V. Yu. Ivanov, and A. M. Balbashov, to be published in Phys. Rev. B (1999)

FIGURES

FIG. 1. Phase diagram of $\text{La}_{1-x}\text{Sr}_x\text{MnO}_3$ from ref. [13]: Structural phases R , O , O' , O'' ; PM = paramagnetic, FM = ferromagnetic, CA = canted antiferromagnetic; M = metallic, I = insulating.

FIG. 2. ESR spectra of $\text{La}_{1-x}\text{Sr}_x\text{MnO}_3$. Left column: various Sr concentrations x at $T = 340$ K ($x = 0.2$ in the rhombohedral R phase, top panel; $x = 0.125$ in the orthorhombic O phase, middle panel; $x = 0.075$ in the strongly distorted orthorhombic O' phase, down panel). Right column: temperature evolution of the ESR spectrum for $x = 0.1$ in three different structural phases. Solid lines represent the fits using the Dysonian line shape, equation 1.

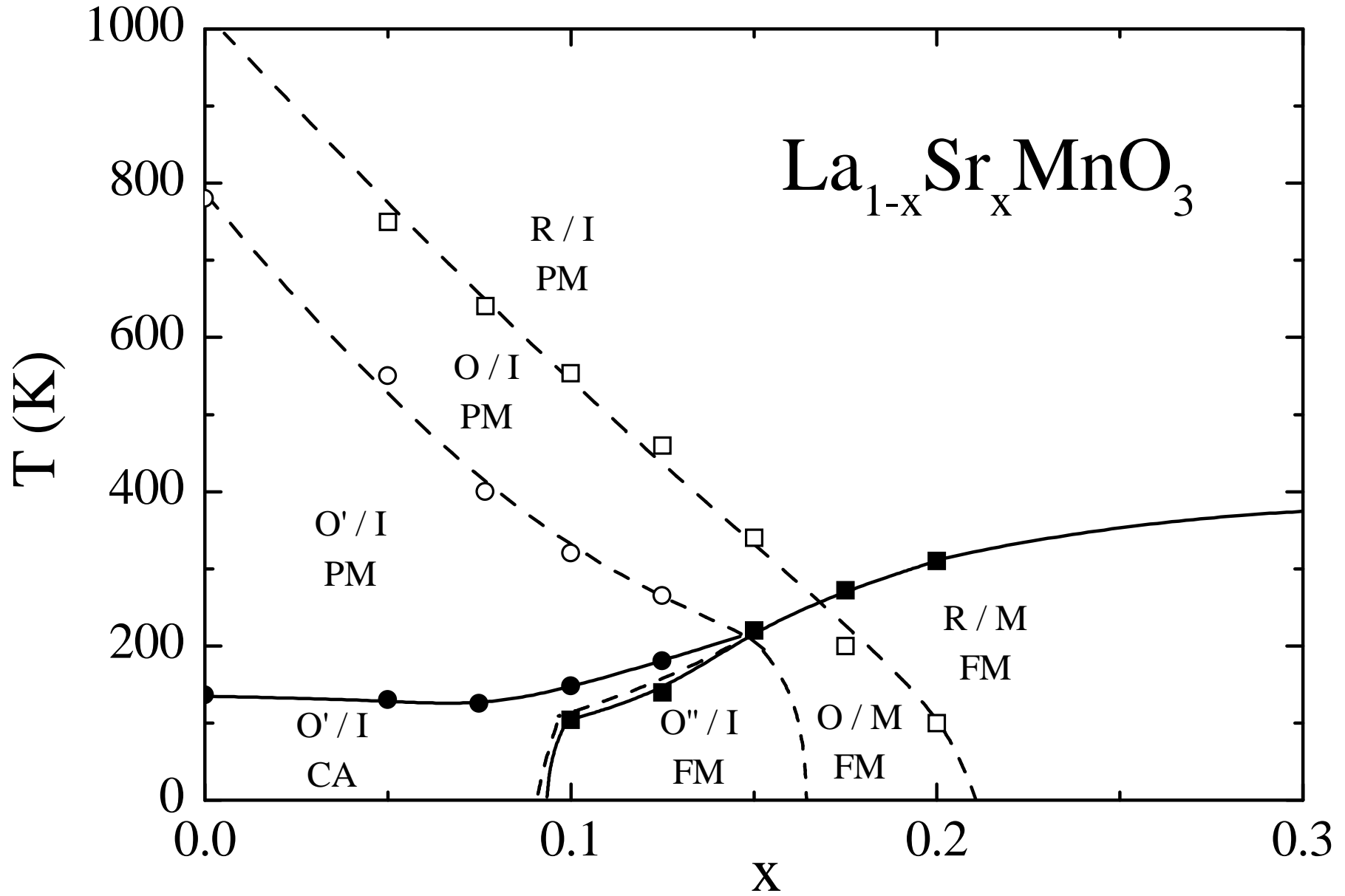
FIG. 3. Temperature dependence of the ESR linewidth ΔH in $\text{La}_{1-x}\text{Sr}_x\text{MnO}_3$ ($0 \leq x \leq 0.2$).

FIG. 4. Temperature dependence of the ESR linewidth in $\text{La}_{0.95}\text{Sr}_{0.05}\text{MnO}_3$ for the three main orientations of H . The insert displays the relative anisotropy.

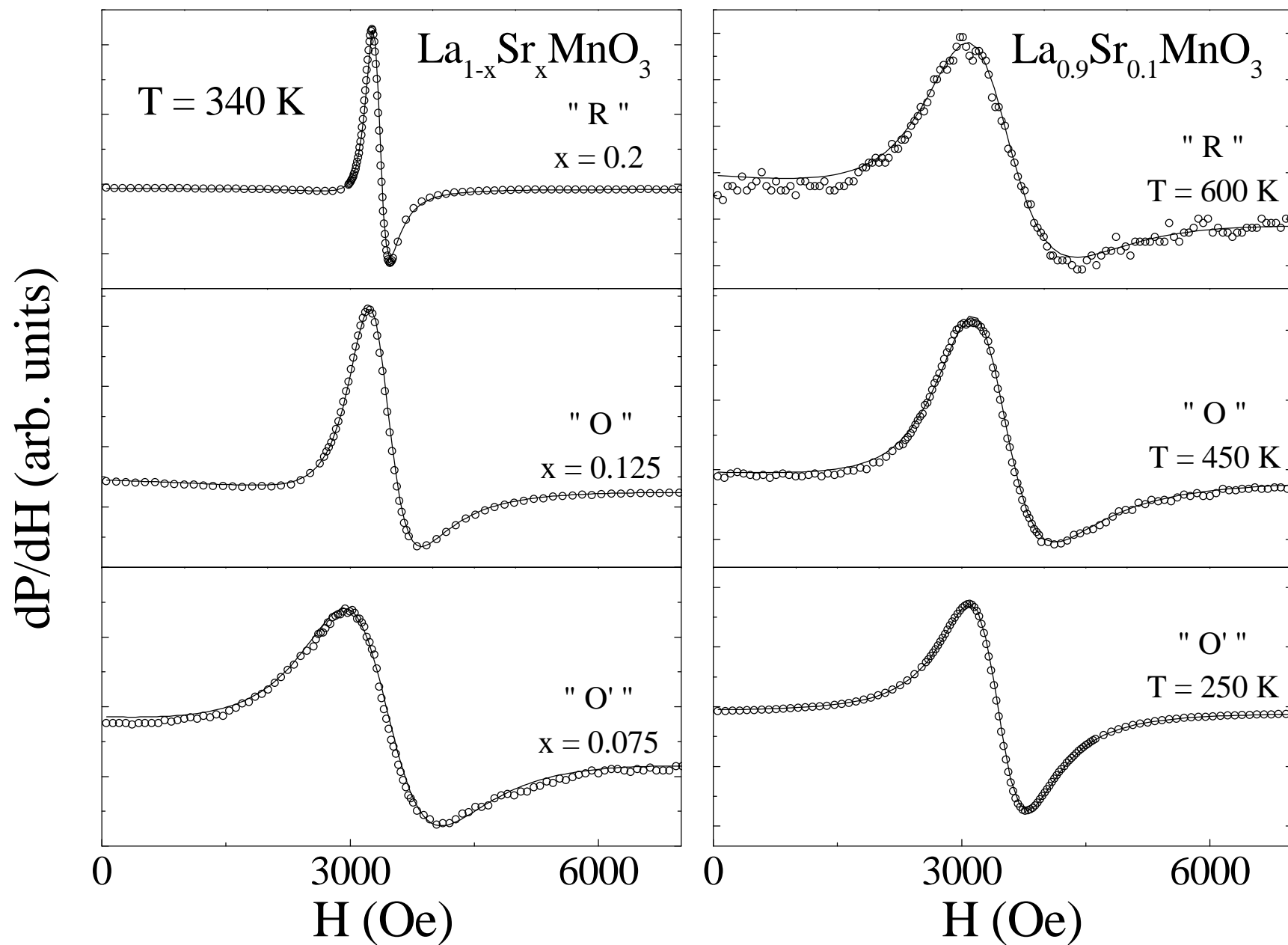
FIG. 5. Angular dependence of the linewidth ΔH in $\text{La}_{0.95}\text{Sr}_{0.05}\text{MnO}_3$ measured at 200 K with external magnetic field $H \perp a$. The solid line represents a fit $A + B \sin^2 \vartheta$ as described in the text. The insert sketches the Jahn-Teller distortion (cf. Fig. 7).

FIG. 6. Reciprocal intensity $1/\chi_{ESR}$ versus temperature in $\text{La}_{1-x}\text{Sr}_x\text{MnO}_3$ for representative Sr concentrations x .

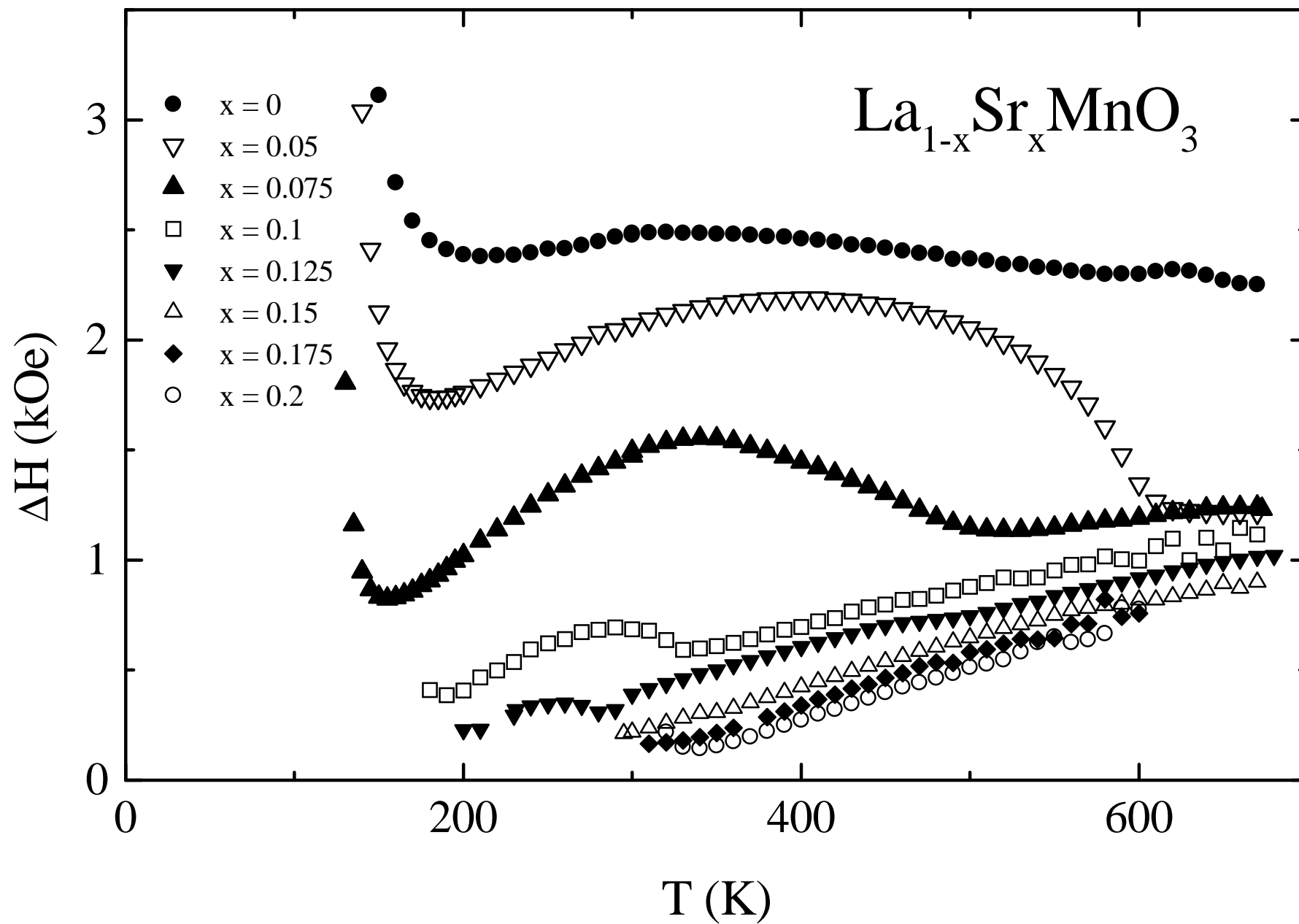
FIG. 7. Crystallographic structure of LaMnO_3 in the strongly Jahn-Teller distorted O' phase [34]. The arrows on the Mn^{3+} ions represent the antiferromagnetic structure below 140 K.



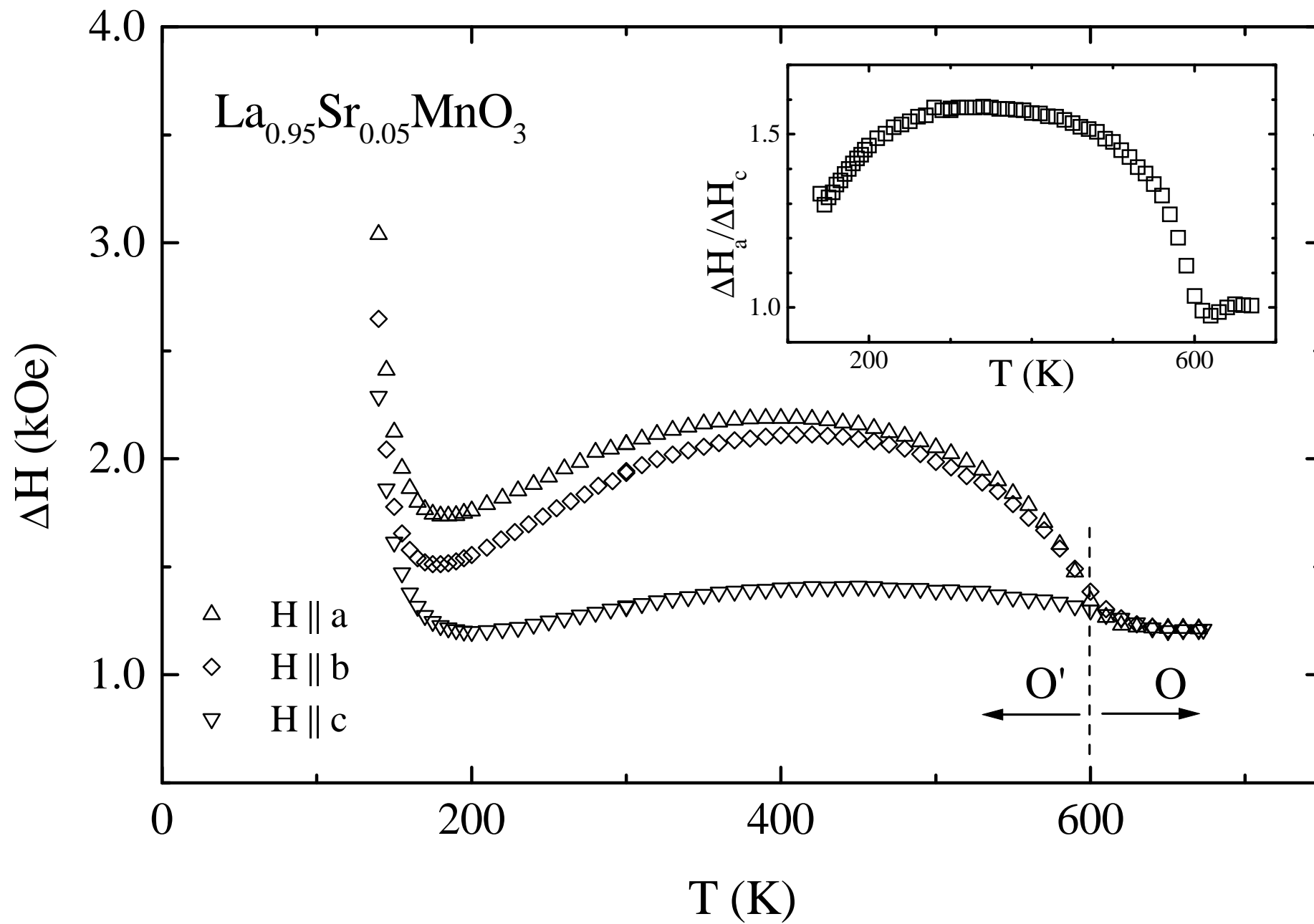
V.A. Ivanshin et al.: Fig. 1



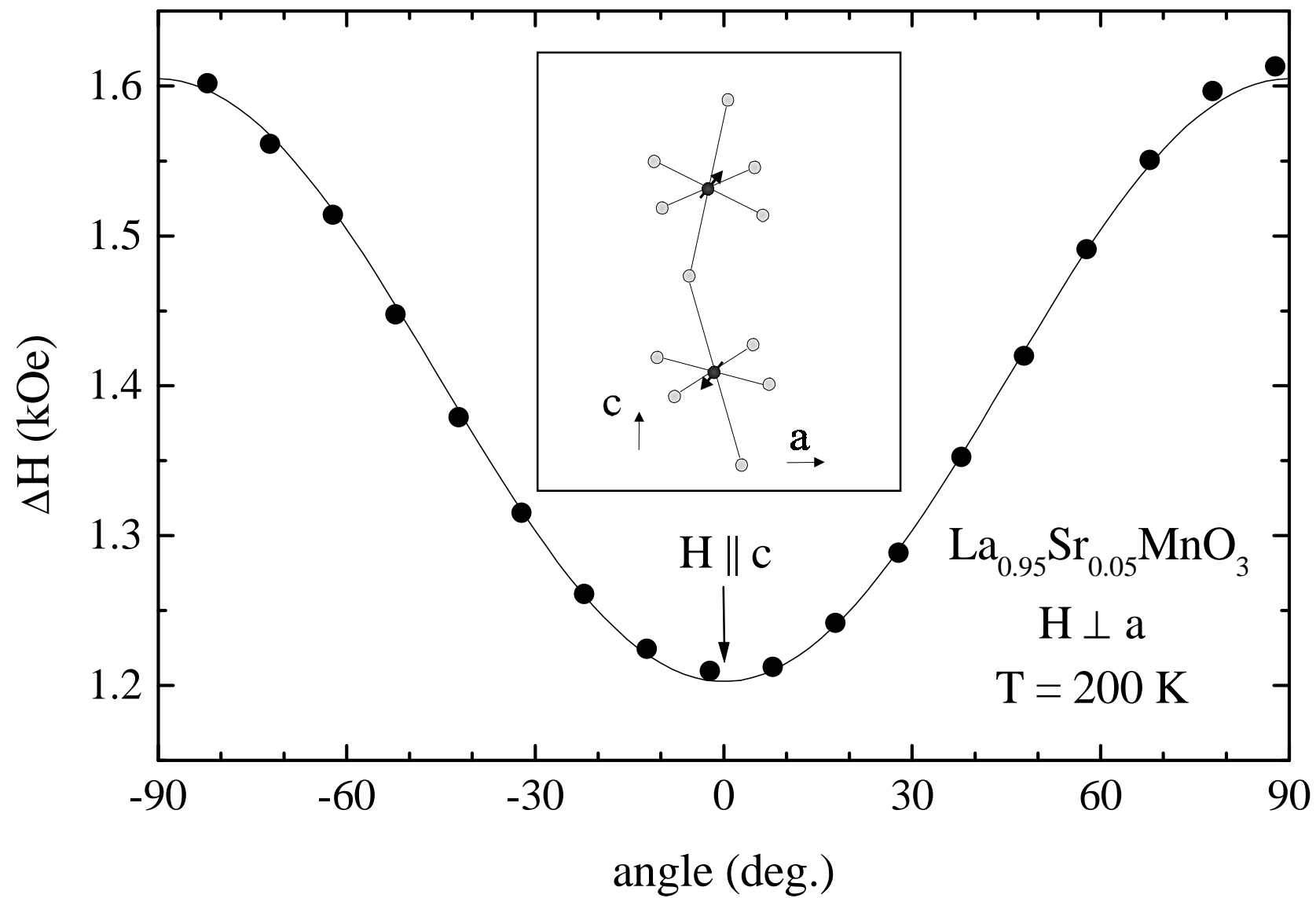
V.A. Ivanshin et al.: Fig. 2



V.A. Ivashin et al.: Fig. 3



V.A. Ivanshin et al.: Fig. 4



V.A. Ivanshin et al.: Fig. 5

